lubricants

MDPI

Article

Compatibility Study of Polyamide (PA6) with Lubricant Bases for Electric Vehicle Applications

Bernardo Tormos [1], Vicente Bermúdez [1], Adbeel Balaguer [1,*] and Enrique Giménez [2]

[1] CMT—Clean Mobility and Thermofluids, Universitat Politècnica de València, 46022 Valencia, Spain; betormos@mot.upv.es (B.T.); bermudez@mot.upv.es (V.B.)
[2] Institute of Materials Technology, Universitat Politècnica de València, 46022 Valencia, Spain; enrique.gimenez@mcm.upv.es
* Correspondence: abalrey@mot.upv.es

Abstract: This study explored the crucial relationship between base fluids and polyamide, a prevalent polymer in electric vehicle (EV) components, with the aim of enhancing the longevity and performance of EVs in the context of thermal management by immersion cooling. Focusing on polyalphaolefin and polyol ester as base fluids, an immersion test was conducted to assess their interaction with polyamide 6 using adapted ASTM standards. The results revealed the significant influences of both fluids on the physical properties and chemical structure of polyamide. Polyol ester demonstrated a lesser impact on the chemical and mechanical properties of polyamide 6.

Keywords: polymer compatibility; immersion cooling; polyol ester oil; polyamide 6

1. Introduction

In the automotive industry, there is a shift towards more sustainable mobility and a rise in electric vehicle use. However, the development of the electric vehicle brings about a series of challenges. One of the most challenging aspects is the thermal management of the vehicle. Thermal management solutions, such as immersion cooling for electric vehicles, require new developments. Additionally, in many powertrains, the lubricant is in contact with the electric motor, and as e-mobility technologies progress, newer designs require lubricants with improved performance attributes.

Traditionally, lubricant specifications for conventional drivetrain systems are mainly focused on generic elastomer tests to evaluate the compatibility of seal materials. Any potential issues related to the compatibility of non-metallic materials were typically identified during hardware component tests and were addressed at a later stage of the development process. However, given the rapid advancements in e-mobility powertrains, it is now prudent to take proactive measures to ensure the compatibility of the fluids with commonly used electric motor components. This proactive approach is essential because, as e-mobility technologies progress, newer designs require fluids with improved performance attributes. In this scenario, E-fluids must be compatible with three principal types of materials: (1) hard plastics, (2) flexible materials, and (3) insulated magnet wire. Hard plastics and flexible materials have structural roles, supporting various motor components such as windings and electrical connectors. A fluid's potential to cause damage lies in its ability to degrade the strength and flexibility of these materials, resulting in weakness or brittleness. This potential can be accurately assessed by subjecting the materials to elevated temperatures for extended periods in the presence of the fluid and subsequently evaluating any changes in mechanical behavior through tensile tests [1].

The electric vehicle (EV) industry faces the challenge of enhancing the performance of EV batteries, including faster charging and discharging rates, increased amp-hour capacity, extended service life, and improved safety. These improvements heavily rely on developing more efficient and safer thermal management solutions. Traditional cooling methods,

Citation: Tormos, B.; Bermúdez, V.; Balaguer, A.; Giménez, E. Compatibility Study of Polyamide (PA6) with Lubricant Bases for Electric Vehicle Applications. *Lubricants* **2024**, *12*, 54. https://doi.org/10.3390/lubricants12020054

Received: 9 January 2024
Revised: 10 February 2024
Accepted: 12 February 2024
Published: 15 February 2024

such as air cooling and indirect liquid cooling (cold plate), have limitations in terms of effectiveness and weight. As an alternative, several automotive manufacturers have recently conducted experiments demonstrating the high efficiency of Single-phase Liquid Immersion Cooling (SLIC) technology for the thermal management of Li-ion batteries [2–5]. In SLIC, the battery is directly immersed in a fluid, enabling direct contact between the battery and the cooling medium [6–9]. This approach offers promising potential as a thermal management solution for EV batteries and the challenge of designing fluids suitable for the application in terms of properties and material compatibility. This paper will aim to delve deeper into that aspect.

Regarding the development of lubricants and battery thermal fluids, the base fluid constitutes a significant portion of the overall composition, typically comprising more than 90% of the fluid volume. On the other hand, additives comprise a smaller fraction [6]. The base fluids serve as the foundation for the formulation, influencing key properties such as viscosity, thermal stability, and electrical conductivity. In this study, we selected polyalphaolefin and polyol ester as base fluids with the potential to be used as bases for the development of e-fluids. This selection is based on the fact that recent studies have demonstrated improved thermal performance of synthetic polyalphaolefins (PAOs) and esters [10,11].

Polyalphaolefins (PAOs) are synthesized through the catalytic oligomerization of alphaolefins, resulting in a saturated oligomeric mixture. This mixture undergoes hydrogenation and distillation processes to yield a range of PAOs. These synthetic fluids are classified based on their viscosities at 100 °C.

PAOs find extensive application as high-performance functional base fluids in various lubricants, including engine lubricants, gear oils, hydraulic oils, automatic transmission oils, compressor/pump oils, and greases. Among these applications, the largest market for PAOs lies in automotive engine (crankcase) lubricants, where they directly compete with petroleum-based oils. Compared to mineral oils, PAOs exhibit several inherent advantages in terms of physical and chemical properties. These advantages include enhanced fluidity at low temperatures, reduced volatility, higher viscosity index, lower pour point, improved oxidative/thermal stability, low toxicity, and biodegradability in the case of low-viscosity grades [12].

Polyol esters (POE) consist of a chain composed of repeating units. Each repeating unit contains an ester functional group, which is formed by the bonding of a carboxylic acid group (–COOH) and an alcohol group (OH). This molecular structure gives polyol esters their unique properties, including thermal stability, oxidative resistance, and lubricating capabilities. They are made by reacting a multifunctional alcohol with a monofunctional acid [13].

Polyamides (PA) are an engineering thermoplastic widely used in automotive, electrical, and electronics applications due to their excellent mechanical properties and chemical resistance. One of the main applications of polyamides in electric vehicles is in the manufacturing of electrical components. Polyamide resins are used to produce connectors, housings, and other components that are critical for the efficient operation of electric powertrains [14]. These components must be able to withstand high temperatures and have excellent electrical insulation properties to prevent shorts and other electrical malfunctions.

The global demand for polyamide resins in the automotive industry is expected to grow significantly in the coming years, driven by the increasing use of lightweight materials in electric vehicles. A report highlights the use of polyamide in electric vehicle battery components [15].

In many of these applications, polyamide is in contact with fluids, which can affect its mechanical properties, reducing its performance. Therefore, understanding the material compatibility between polyamide and the fluid is essential to ensuring the longevity and optimal performance of the application.

Some studies have been conducted to analyze material compatibility between elastomers or plastic and automotive fluids. For example, Durbin et al. studied the compati-

bility of different materials exposed to ethanol and butanol blends by tensile test [16]. A similar approach to the material compatibility of elastomer sealing O-rings was carried out, and permanent changes were found by the tests. The degradation of elastomer O-rings was more pronounced for the tested fuels containing ethanol, iso-butanol, n-butanol, methanol, and dodecanol [17].

Another study focused on the theoretical analysis and experimental investigation of material compatibility between refrigerants and polymers. A lubricant polyester was also included in that study, and the compatibility tests were conducted between 25 and 75 °C [18]. These studies are focused on vehicles powered by fossil fuels.

As previously mentioned, electric motors introduce several different polymers in the form of magnet wire insulation, flexible sheets, elastic bindings, and hard plastics. However, there is currently a standardized testing method for evaluating these components. The current state of testing is discussed in SAE J3200 [1], and other reputable sources such as STLE also comment on the actual state of test methods for the evaluation of electric vehicle drivetrain fluids, suggesting adaptations of existing ASTM standards to this new application [19].

Ensuring the compatibility of materials is pivotal for the reliable performance and longevity of electric vehicles. This study focused on investigating the interaction between polyamide 6, a widely utilized polymer, and two essential base fluids, polyalphaolefin and polyol ester. Our research employs an immersion test, adapted from ASTM Standard D7216 [20], to rigorously evaluate the compatibility between polyamide 6 and the selected base fluids within the context of EV applications.

Additionally, a detailed chemistry characterization of the polymer after immersion was conducted to elucidate the underlying effects of the fluids on polyamide 6. By unraveling the changes induced by fluid exposure, this study aims to provide fundamental insights into material compatibility in electric vehicles.

2. Materials and Methods

2.1. Materials

Polyamide 6 (PA6):

Polyamides are linear polymers with repeating units linked by amide bonds, characterized by highly precise block lengths and well-defined block sequences within the polymer chain. In this study, we selected polyamide 6; the number represents the number of carbon atoms present in the amino carboxylic acid (6 in this case) [21].

For the research, sheets with a thickness of 2 mm were procured from Sigma-Aldrich, Madrid, Spain. The required shapes for the test specimens were subsequently fabricated by cutting them from these sheets.

Linear formula: $[\text{-NH}(\text{CH}_2)_5\text{CO-}]_n$

Structural formula:

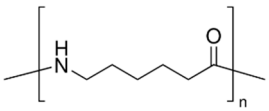

Base fluids:

In the present study, the base fluids utilized were not mixed with additives and were used in their pure form. After considering previous studies [10,11], two base fluids were selected for the study: a polyalphaolefin (PAO) and a polyol ester (POE).

For this study, PAO 4 was used, which means that it has a viscosity of 4 cst at 100 °C. Specifically, SpectraSyn 4 polyalphaolefin fluid from ExxonMobile.

As a polyol ester, we used Waglinol 3/13480 from IQLubricants, which is a low-viscosity, oxidative-stable, low deposit-forming polyol ester. Additionally, it has a high viscosity index and is biodegradable. The viscosity information for the fluids is provided in Table 1.

Table 1. Kinematic viscosity (**ν**) and viscosity index of the fluids used.

Fluid	ν 40 °C	ν 100 °C	Viscosity Index
PAO	17.90 mm²/s	4.03 mm²/s	125
POE	19.84 mm²/s	4.45 mm²/s	140

2.2. Methods

The compatibility between the polyamide and the lubricant bases was studied by means of an immersion test. An immersion test is an operation to evaluate compatibility by determining the effect of a liquid on test specimens submerged in the liquid for a specified time and at a specified temperature. The effect of the liquid is evaluated by the difference in the test material's physical properties pre- and post-immersion.

The immersion tests were adapted from ASTM D7216 [20], with testing temperatures of 20 °C (room temperature), 90 °C, and 120 °C. In line with the requirements of electric vehicle applications, we implemented temperatures lower than those prescribed by the standard. Moreover, the test tube arrangement was adapted by employing a 1 L beaker instead of a smaller glass tube. This modification facilitated the inclusion of probes necessary for the tensile testing of plastics.

Polyamide samples were completely immersed in a beaker and maintained at the corresponding temperature for a total of 168 h (one week). This study evaluated two combinations of polymer and base fluid (PA6—PAO4; PA6—POE) at three different temperatures.

Measurements of the initial mass, hardness Shore D, and tensile test were made on samples obtained from PA6 sheets.

Five samples, type I according to ASTM D638 [22], were used for tensile measurements, and five specimens measuring 2 × 5 cm were used for mass and hardness measurements. Heating was performed in a thermal bath. Lids were used to cover the beakers to reduce evaporation and prevent contamination.

2.2.1. Measurement of Mass Changes

To quantify this property, five specimens of PA6 were used for each combination of fluid (PAO4; POE) and temperature (20 °C, 90 °C, and 120 °C). Then, the mean value for each of the six tests was calculated.

In each case, the mass of each specimen was recorded before and after heating using an analytical balance (KERN 770) with a readability of 0.0001 g.

For each test (combination of PA6/test oil/temperature), the change in properties was calculated as follows:

$$\Delta mass = 100\left[\left(m_f - m_i\right)/m_i\right] \quad (1)$$

where:

$\Delta mass$: mass change, %
m_f: final mass, g
m_i: initial mass, g

2.2.2. Measurement of Hardness Changes

The hardness of each sample was recorded before and after immersion in the fluid in order to calculate the hardness change. For each one, six measurements were taken on each specimen using a Shore D durometer, and the arithmetic mean was calculated. The specimens were plied to obtain the necessary thickness (6 mm) following the ASTM D2240 [23].

For each test (combination of PA6/base fluid/temperature), the change in properties was calculated as follows:

$$\Delta H = \left(H_f - H_i\right)/H_i \quad (2)$$

where:

ΔH: hardness change, Shore D units

H_f: final hardness, Shore D units
H_i: initial mass, Shore D units

2.2.3. Measurement of Tensile Strength and Elongation Changes

The tensile strength, or the maximum tensile stress applied in stretching a specimen to rupture, and the ultimate elongation, or the elongation at which rupture occurs in the application of continued tensile stress, were recorded. The tensile strength and ultimate elongation measurements were carried out according to ASTM D638 [22] using tensile test dumbbell specimens (type I) and a test speed of 5 mm/min (see Figure 1).

Figure 1. Tensile testing machine used and polyamide dumbbells for testing.

The tensile strength and elongation for each combination of base fluid/temperature were measured on five specimens, and their average values were reported. PA6 samples without immersion in the oil fluids were also tested to a comparative effect. All measures were carried out in the same environmental conditions.

For each test (combination of PA6/test oil/temperature), the change in properties was calculated as follows, according to ASTM D7216 [20]:

$$\Delta E = 100\left[\left(E_f - E_i\right)/E_i\right] \quad (3)$$

where:
ΔE: ultimate elongation change, %
E_f: final ultimate elongation, g
E_i: initial ultimate elongation, g
And analogously for the tensile strength.

2.2.4. Fourier Transform Infrared of Polyamide—FTIR

Additionally, spectrometric analyses were conducted to obtain a more comprehensive understanding of the compatibility between the materials. The polyamide was analyzed before and after the immersion tests to detect possible changes in the material.

PA6 samples exposed to oil fluids at 90 °C and 120° C were analyzed by Fourier Transform Infrared Spectroscopy using an Attenuated Total Reflection measurement accessory (ATR-FTIR spectroscopy, FT/IR-6200 Jasco, Valencia, Spain) in order to study the chemical changes during the exposition. The FTIR spectra were acquired in the spectral window of 4000 to 400 cm^{-1} at a resolution of 4 cm^{-1} with 150 accumulations in ATR mode. All

the infrared spectra were processed through an ATR correction and subsequent multiple points baseline correction.

2.2.5. Crystallinity

The crystallinity of virgin PA6 and PA6 immersed in the base fluids was determined by differential scanning calorimetry (DSC, TA, Q100) at a scanning rate of 10 °C min^{-1} from 20 to 250 °C under a nitrogen atmosphere. A heat of fusion value of 184 J g^{-1} for 100% crystalline polyamide 6 was used in the calculation of the mass crystallinity [24]. The crystallinity of samples was calculated according to the following Equation (4):

$$\% \, Crystallinity = \frac{\Delta H_{f-} \Delta H_c}{\Delta H_f^0} \times 100\% \quad (4)$$

where ΔH is the measured heat of fusion, ΔH_c is the cold crystallization enthalpy and is the 100% crystalline heat of fusion.

2.2.6. X-ray Diffraction—XRD

The X-ray diffraction scans were made for the nondegraded PA6 sample and for the samples subjected to the immersion test at 120 °C.

The XRD measurements were performed on 2D Phaser equipment (Bruker, Madrid, Spain) with Cu-K radiation working at 30 kV and 10 mA in order to determine changes in the crystalline structure of PA6.

3. Results

3.1. Mass Change

The mass before immersion in the base fluid is compared with the mass after the testing to obtain the mass change value according to Equation 1, and the results are shown in Figure 2. It can be seen that the effects on the mass are greater with temperature, and there was a mass loss slightly bigger for the samples in contact with polyol ester. For both base fluids, the magnitude is similar—around 2%. For the specimens that remained submerged at ambient temperature, the mass change was insignificant since the value is similar to the tolerance error of the balance.

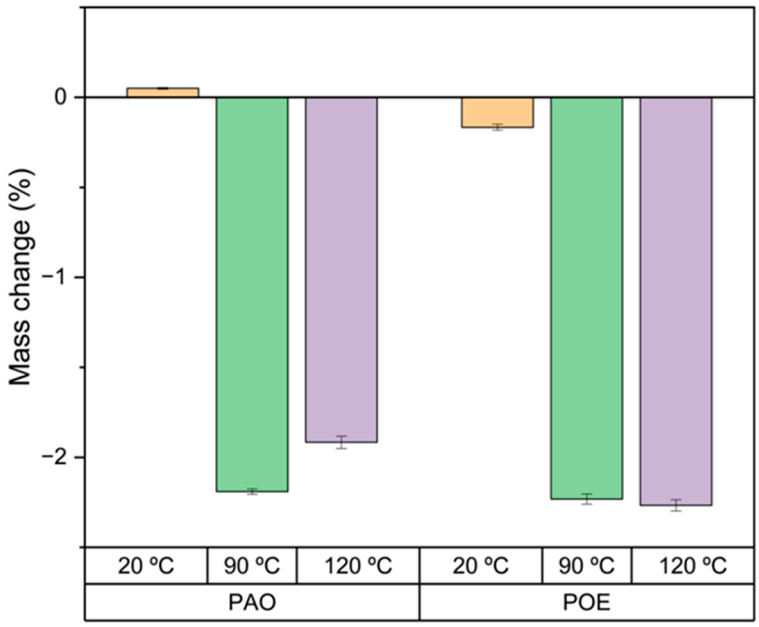

Figure 2. Mass change.

3.2. Hardness Change

The hardness variation of the specimens subjected to the immersion test is depicted in Figure 3. The reported values were rounded to the nearest whole Shore D points, following ASTM D7216 guidelines. There was no significant variation in hardness for the specimens kept at room temperature. The initial hardness value for the polyamide without immersion was 76 Shore D points. However, the specimens maintained at 90 and 120 °C experienced a hardening of 4 to 6 points on the Shore D scale. The most pronounced change of 6 points was observed in the specimens in contact with PAO at 120 °C.

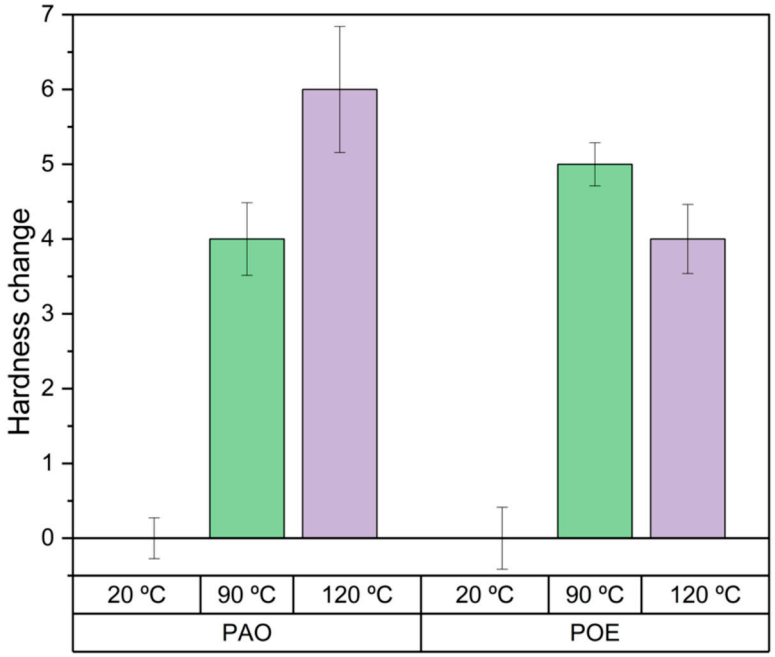

Figure 3. Hardness change expressed in Shore D points.

The observed increase in hardness of the specimens subjected to the immersion test may be attributed to a process of crosslinking [18,25]. Crosslinking refers to the formation of chemical bonds between polymer chains; as a result, the polymer chains become interconnected, forming a network structure that restricts molecular mobility and imparts increased rigidity to the material. This process can lead to an enhancement in the material's hardness and brittleness, accompanied by reduced elongation and poorer tensile strength values.

Furthermore, in the case of thermoplastics, including polyamides, the interaction between the fluid medium and the polymer can also influence the degree of crystallization. The presence of a fluid, such as polyalphaolefin (PAO) in this study, can promote crystallization in polyamides, leading to an increase in hardness.

3.3. Tensile Test

The tensile strength represents the maximum tensile stress endured by a specimen until rupture. Table 2 lists the average values obtained for the mechanical properties of the materials for each test. In our study, we observed a decrease in tensile strength for specimens exposed to both fluids at room temperature in comparison to the PA6 specimens without immersion. Specifically, specimens in contact with PAO experienced an 8.85% reduction in tensile strength, whereas those in contact with POE exhibited a 5.52% decrease. When the specimens were immersed at 90 °C, both fluids led to a similar increase in the tensile strength, as shown in Tables 2 and 3. However, at 120 °C, the behavior diverged. For the specimens immersed in PAO, the maximum tensile strength increased by only 9.95%, and they fractured without undergoing elastic deformation, as depicted in Figure 4. In contrast, the specimens immersed in POE experienced a more significant change, with a

19.63% increase in tensile strength, as evident from the corresponding curve in Figure 5, where they underwent elastic deformation before reaching the breaking point.

Table 2. Effect of temperature on mechanical properties of PA6 immersed in the base fluids.

Temp.	PA6 w/o Immersion	PA6 Immersed PAO			PA6 Immersed POE		
		20 °C	90 °C	120 °C	20 °C	90 °C	120 °C
Tensile strength (MPa)	63.74 ± 1.28	58.10 ± 2.09	74.97 ± 0.43	70.08 ± 4.66	60.22 ± 3.21	75.69 ± 0.72	76.25 ± 0.13
Strain at break (%)	31.71 ± 1.92	158.78 ± 13.76	21.70 ± 1.91	3.52 ± 0.45	163.43 ± 13.39	24.79 ± 1.69	23.27 ± 2.09

Table 3. Percentage of change for the tensile strength and ultimate elongation.

Immersion Temp.	PA6 Immersed PAO			PA6 Immersed POE		
	20 °C	90 °C	120 °C	20 °C	90 °C	120 °C
Tensile strength change (%)	−8.85	17.62	9.95	−5.52	18.75	19.63
Ultimate elongation change (%)	400.73	−31.57	−88.90	415.39	−21.82	−26.62

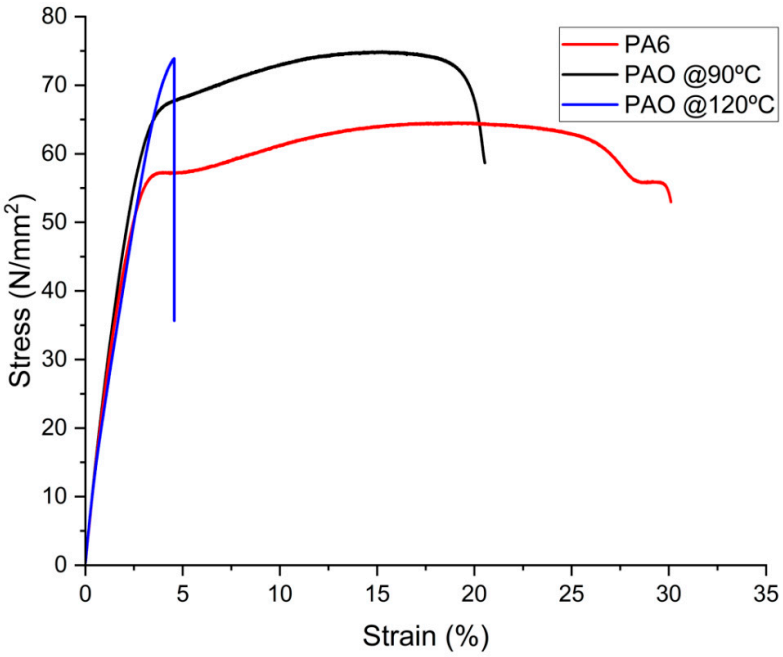

Figure 4. Effect of temperature on tensile curves for PA6 immersed in PAO.

Ultimate elongation, which represents the point at which rupture occurs under continuous tensile stress, is a critical mechanical property to consider. Tables 2 and 3 provide insights into the effect of immersion in different fluids and temperatures on this property in PA6 specimens.

At room temperature (20 °C), both sets of immersed specimens exhibited a 400% increase in elongation capacity compared with the original PA6 specimens, highlighting a substantial change in polymer elasticity due to fluid contact.

In the case of temperature-applied immersion, the most significant alteration occurred with specimens exposed to PAO at 120 °C, showing a drastic 88.90% reduction in ultimate elongation compared to the reference polyamide samples. Similarly, at 90 °C, a notable decrease of 31.57% was observed. In contrast, the specimens in contact with POE showed a less significant reduction, with ultimate elongation decreases of 21.86% at 90 °C and 26.62% at 120 °C.

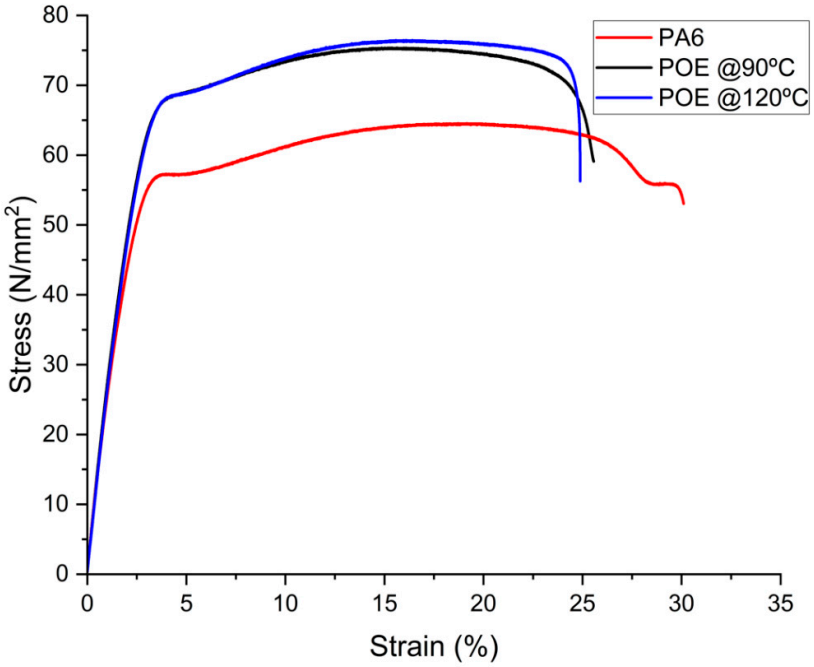

Figure 5. Effect of temperature on tensile curves for PA6 immersed in POE.

Figures 4 and 5 depict the strain–stress curves for the tests conducted at 90 and 120 °C for both fluids. The red curve represents the elongation of the reference polyamide specimens that were not subjected to immersion. It is evident from these curves that the specimens in contact with PAO experienced a greater reduction in elasticity, with the specimens at 120 °C even fracturing before undergoing plastic deformation.

These findings suggest that the immersion of polyamide 6 specimens in PAO at elevated temperatures significantly diminishes their elongation properties and overall ductility.

3.4. Color Change

After the experimental period, notable color variations were observed on the surface of the polymer samples. The accompanying images, Figures 6 and 7, illustrate the distinct changes in color that occurred as a result of the immersion process. These visual transformations provide insights into the interaction between the polymer matrix and the surrounding medium.

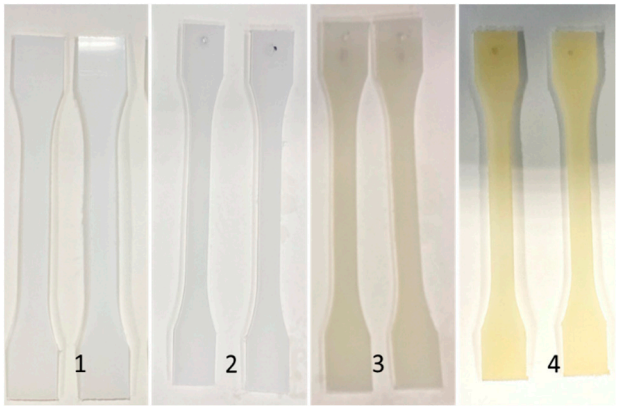

Figure 6. Color change for PA6 original (1) and immersed in POE at 20 °C (2), 90 °C (3), and 120 °C (4).

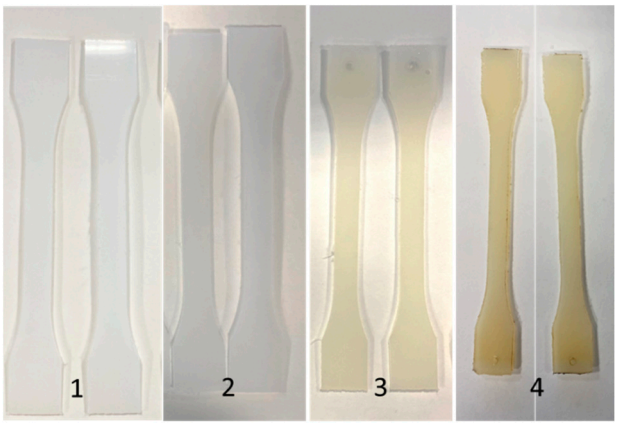

Figure 7. Color change for PA6 original (1) and immersed in PAO at 20 °C (2), 90 °C (3), and 120 °C (4).

3.5. Chemistry Characterization

3.5.1. Fourier Transform Infrared of Polyamide—FTIR

FTIR can help monitor the degradation of the polymer functional groups and chemical bonds changed throughout the aging evolution, which could be monitored by spectral analysis [25].

PA6 samples exposed to oil fluids at 90 °C and 120° and unexposed PA6 were analyzed by Fourier Transform Infrared Spectroscopy in order to study the chemical changes during the artificial exposition, and the results are shown in Figure 8. The spectrum for PA6 resin shows characteristic absorption bands of hydrogen-bonded NH stretching (3289 cm^{-1}), C–H asymmetric of CH_3 (2921 cm^{-1}), C-H symmetric of CH_2 (2853 cm^{-1}), Amide I and C=O stretching (1630 cm^{-1}), and Amide II and the mixed motions of C–N stretching and N-H in-plane bending vibration (1541 cm^{-1}) [26–29].

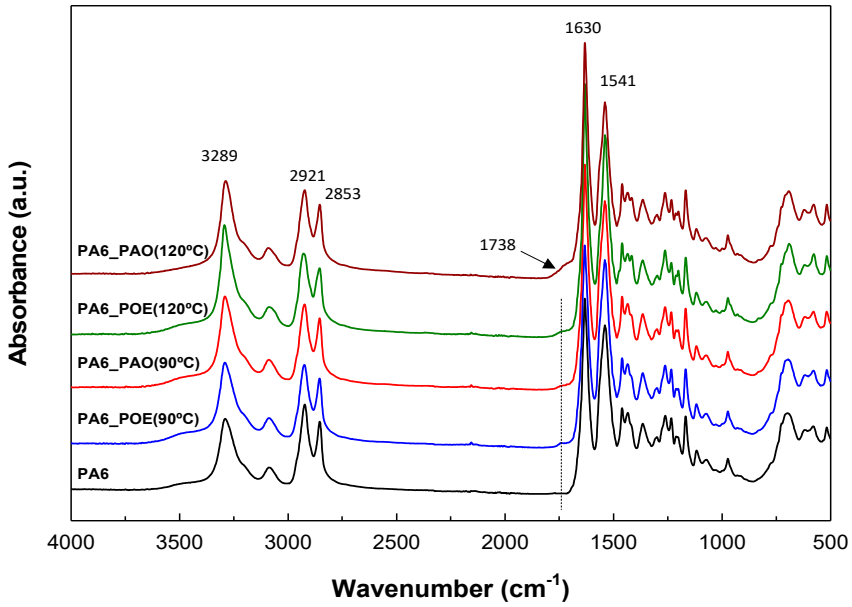

Figure 8. FTIR spectra of the studied polyamide samples.

Figure 9 shows a magnified view of the carbonyl species region (1850 ~ 1500 cm^{-1}) of ATR-IR spectra. A progressive increase in the absorption intensity and a notable shoulder was observed for the PA6 samples immersed in the base fluids (PAO and POE), with absorption maxima at 120 °C. With increasing temperature, the shoulder peak at 1738 cm^{-1} became more evident, and the Amide I peak (1630 cm^{-1}) also increased. These changes were higher in the PAO fluid, which were due to the formation of carbonyl groups on

the sample surface during the immersion process, indicating a certain thermo-oxidative degradation of polyamide 6 [30].

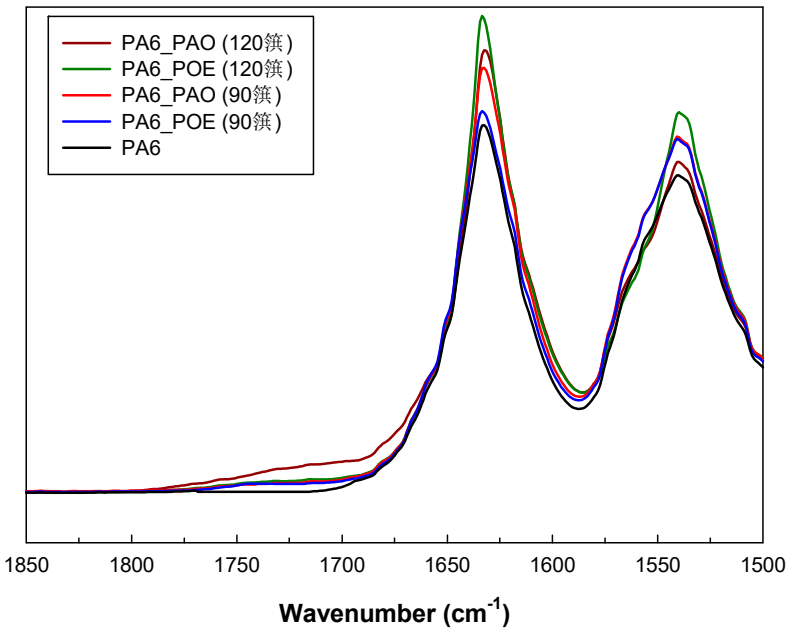

Figure 9. Magnified view of the carbonyl species region (1850–1500 cm^{-1}).

3.5.2. X-ray Diffraction—XRD

X-ray diffraction (XRD) patterns have been utilized to assess the degree of ordering within polymers during the aging process. By examining the diverse compositions of the crystalline and amorphous phases, as well as changes in crystallinity, valuable insights can be gained [25].

The X-ray diffraction patterns of neat polyamide 6, as well as the PA6 after exposure to PAO and POE at 120 °C, are shown in Figure 10 for the 2θ range from 10 to 35°. The X-ray diffraction patterns reveal the presence of two polymorphs coexisting in neat PA6. A prominent peak at 2θ = 21.5° associated with the γ phase (pseudo-hexagonal) and two surrounding shoulder peaks at 2θ = 20.3° and 23.4° corresponding to the α phase (monoclinic) are attributed to the reflections from the (200) and (002, 202) planes.

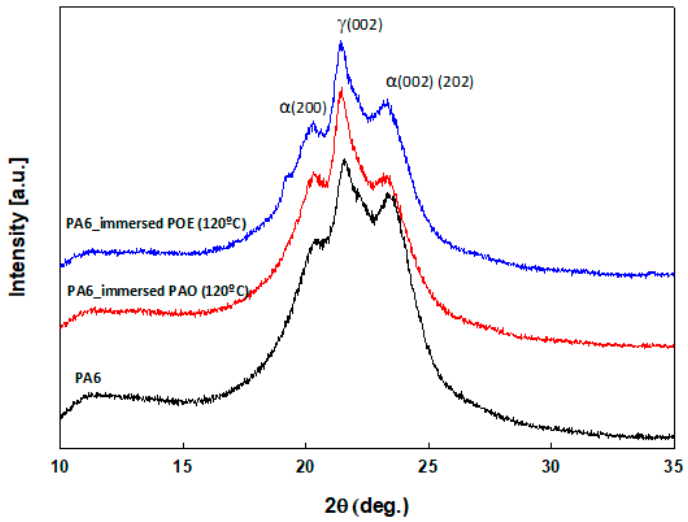

Figure 10. X-ray diffraction scans of the studied polyamide samples.

The γ phase is thermodynamically less stable compared to the α phase due to the less efficient hydrogen bonding between the parallel chain arrangement, as the chains are not as close together or as aligned as in the α phase [24].

In the case of PA6 samples immersed in the base fluids (PAO and POE) at 120 °C, the dominant crystalline structure associated with γ-form crystals remains unchanged. However, the peaks corresponding to the α phase at 2θ = 20.3° show a slight increase in intensity, indicating the formation of more stable crystals due to the annealing, as also confirmed by measurements of crystallinity degree determined by DSC.

3.5.3. Crystallinity

The crystallinity of the virgin PA6 and the samples immersed in fluids at elevated temperatures was calculated according to Section 2.2. The results are presented in Figure 11, where it is evident that the fluid–polymer interaction influenced the degree of crystallization. The fluids in contact with PAO exhibited a higher degree of crystallinity compared to the samples immersed in POE. And an increase in crystallization would cause an increase in the hardness of the material [18], which is congruent with the results obtained in Section 3.2.

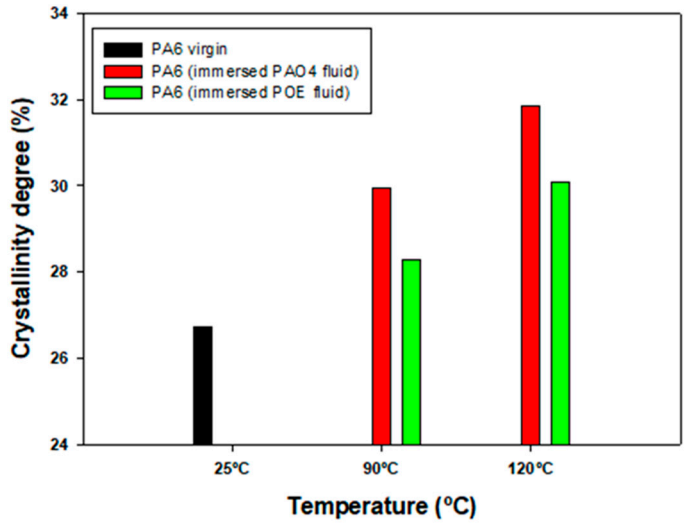

Figure 11. Crystallinity degree.

4. Conclusions

This study aimed to compare the effects of two different fluids on polyamide through an immersion test, as detailed in the Methods section. The results unequivocally demonstrate that both fluids significantly influence the physical properties and chemical structure of polyamide. Remarkably, our findings indicate that POE has a comparatively lesser impact on the chemical and mechanical properties of polyamide, making polyol esters more promising candidates as base oils for developing fluids tailored for thermal management in battery electric vehicles.

However, it is crucial to emphasize that apart from compatibility, several other facets, such as thermal and electrical properties, need meticulous consideration. Addressing these aspects is imperative to ensuring the optimal functioning of the developed fluids in real-world applications, especially in electric vehicle systems where thermal management plays a pivotal role in efficiency and longevity.

Additionally, it is worth noting that the conducted tests focused solely on the base fluid. Considering the complexity of practical applications, it is highly probable that additive inclusion might be necessary. Future research endeavors should delve into the effects of additive inclusion and its potential implications on overall performance. This comprehensive analysis is vital to fine-tuning the formulation, ensuring both optimal performance and durability in electric vehicle systems.

In light of these findings, it is evident that developing effective thermal management fluids for battery electric vehicles involves a multifaceted approach. Beyond compatibility, a thorough understanding of thermal and electrical properties, coupled with the intricate interplay of additives, is indispensable. Further research and validation are indispensable to exploring the long-term effects comprehensively, paving the way for the optimization of formulations and the realization of efficient and durable thermal management solutions for the evolving demands of electric vehicle technologies.

Author Contributions: Conceptualization, B.T. and E.G.; Formal analysis, A.B. and E.G.; Funding acquisition, V.B.; Investigation, A.B.; Methodology, B.T. and A.B.; Project administration, V.B.; Resources, V.B.; Supervision, B.T.; Writing—original draft, A.B.; Writing—review and editing, B.T. and E.G. All authors have read and agreed to the published version of the manuscript.

Funding: This research was partly supported by the project CIAICO/2021/013 AICO 2022 funded by GVA, Generalitat Valenciana. Adbeel Balaguer is supported through the program Subvenciones para la contratación de personal investigador predoctoral of the Generalitat Valenciana and the European Social Fund Plus [grant number CIACIF/2021/241].

Data Availability Statement: Data are contained within the article.

Conflicts of Interest: The authors declare no conflicts of interest. The funders had no role in the design of the study, in the collection, analyses, or interpretation of data, in the writing of the manuscript; or in the decision to publish the results.

References

1. Fuels and Lubricants TC 3 Driveline and Chassis Lubrication, Fluid for Automotive Electrified Drivetrains, 2022. Available online: https://www.sae.org/standards/content/J3200_202210/ (accessed on 15 May 2023).
2. Rémi, D.; Juhasz, J.R. Assessment of immersion cooling fluids for electric vehicle battery thermal management. In Proceedings of the 32nd Electric Vehicle Symposium (EVS32), Lyon, France, 19–22 May 2019.
3. Immersed-Cooling Concepts for Electric Vehicle Battery Packs Using Viscoelastic Heat Transfer Liquids (I-BAT) | I-BAT | Project | Fact sheet | H2020 | CORDIS | European Commission. Available online: https://cordis.europa.eu/project/id/899659 (accessed on 4 December 2023).
4. Sundin, D.W.; Sponholtz, S. Thermal management of Li-ion batteries with single-phase liquid immersion cooling. *IEEE Open J. Veh. Technol.* **2020**, *1*, 82–92. [CrossRef]
5. Williams, N.P.; Trimble, D.; O'Shaughnessy, S.M. Thermal Management of Lithium-ion Batteries for Electric Vehicles through Immersion Cooling. In Proceedings of the 22nd InterSociety Conference on Thermal and Thermomechanical Phenomena in Electronic Systems, ITHERM, Orlando, FL, USA, 30 May–2 June 2023. [CrossRef]
6. Narita, K.; Takekawa, D. *Lubricants Technology Applied to Transmissions in Hybrid Electric Vehicles and Electric Vehicles, SAE Technical Papers*; SAE International: Warrendale, PA, USA, 2019. [CrossRef]
7. Patil, M.S.; Seo, J.H.; Lee, M.Y. A novel dielectric fluid immersion cooling technology for Li-ion battery thermal management. *Energy Convers Manag.* **2021**, *229*, 113715. [CrossRef]
8. Roe, C.; Feng, X.; White, G.; Li, R.; Wang, H.; Rui, X.; Li, C.; Zhang, F.; Null, V.; Parkes, M.; et al. Immersion cooling for lithium-ion batteries – A review. *J. Power Sources* **2022**, *525*, 231094. [CrossRef]
9. Tormos, B.; Bermúdez, V.; Ruiz, S.; Alvis-Sanchez, J. Degradation Effects of Base Oils after Thermal and Electrical Aging for EV Thermal Fluid Applications. *Lubricants* **2023**, *11*, 241. [CrossRef]
10. Szewczyk, R.; Wicks, R.; Martin, R. Comparison of Synthetic and Natural Esters with Focus on Thermal Aspects of Insulation Systems. In Proceedings of the CIRED 2021—The 26th International Conference and Exhibition on Electricity Distribution, Virtual Event, 20–23 September 2021; pp. 142–146.
11. Narvaez, J. Thermal Conductivity of Poly-alpha-olefin (pao)-Based Nanofluids. Master's Thesis, University of Dayton, Dayton, OH, USA, 2010.
12. Benda, R.; Bullen, J.; Plomer, A. Synthetics basics: Polyalphaolefins–Base fluids for high-performance lubricants. *J. Synth. Lubr.* **1996**, *13*, 41–57. [CrossRef]
13. Lin, L.; Kedzierski, M.A. Density and viscosity of a polyol ester lubricant: Measurement and molecular dynamics simulation. *Int. J. Refrig.* **2020**, *118*, 188–201. [CrossRef] [PubMed]
14. Kondo, M.Y.; Montagna, L.S.; Morgado GF, D.M.; Castilho AL, G.D.; Batista LA PD, S.; Botelho, E.C.; Costa, M.L.; Passador, F.R.; Rezende, M.C.; Ribeiro, M.V. Recent advances in the use of Polyamide-based materials for the automotive industry. *Polímeros* **2022**, *32*. [CrossRef]
15. Global $53.32 Billion Polyamide Markets to 2028. Available online: https://www.globenewswire.com/news-release/2021/10/22/2319003/28124/en/Global-53-32-Billion-Polyamide-Markets-to-2028-Increasing-Demand-from-the-Automobile-Industry-Growing-Demand-from-End-use-Industries.html (accessed on 15 April 2023).

16. Durbin, T.D.; Karavalakis, G.; Norbeck, J.M.; Park, C.S.; Castillo, J.; Rheem, Y.; Bumiller, K.; Yang, J.; Van, V.; Hunter, K. Material compatibility evaluation for elastomers, plastics, and metals exposed to ethanol and butanol blends. *Fuel* **2016**, *163*, 248–259. [CrossRef]
17. Müller, M.; Šleger, V.; Čedík, J.; Pexa, M. Research on the Material Compatibility of Elastomer Sealing O-Rings. *Polymers* **2022**, *14*, 3323. [CrossRef] [PubMed]
18. Eyerer, S.; Eyerer, P.; Eicheldinger, M.; Tübke, B.; Wieland, C.; Spliethoff, H. Theoretical analysis and experimental investigation of material compatibility between refrigerants and polymers. *Energy* **2018**, *163*, 782–799. [CrossRef]
19. McGuire, N. *Test Methods for Evaluation of Electric Vehicle Drivetrain Fluids*; Society of Tribologists and Lubrication Engineers—STLE: Park Ridge, IL, USA, 2023.
20. *ASTM D7216*; Standard Test Method for Determining Automotive Engine Oil Compatibility with Typical Seal Elastomers. ASTM International: West Conshohocken, PA, USA, 2023.
21. Baldi, L.D.; Iamazaki, E.T.; Atvars, T.D. Evaluation of the polarity of polyamide surfaces using the fluorescence emission of pyrene. *Dye. Pigment.* **2008**, *76*, 669–676. [CrossRef]
22. *ASTM D638*; Standard Test Method for Tensile Properties of Plastics. ASTM International: West Conshohocken, PA, USA, 2022.
23. *ASTM D2240*; Standard Test Method for Rubber Property—Durometer Hardness. ASTM International: West Conshohocken, PA, USA, 2021.
24. Bandrup, J.; Immergut, E. *Polymer Handbook*, 3rd ed.; John Wiley and Sons: Hoboken, NJ, USA, 1989.
25. Tian, R.; Li, K.; Lin, Y.; Lu, C.; Duan, X. Characterization Techniques of Polymer Aging: From Beginning to End. *Chem. Rev.* **2023**, *123*, 3007–3088. [CrossRef] [PubMed]
26. Palmer, R.J. Polyamides, Plastics. In *Kirk-Othmer Encyclopedia of Chemical Technology*; Wiley: Hoboken, NJ, USA, 2005. [CrossRef]
27. Shi, K.; Ye, L.; Li, G. Thermal oxidative aging behavior and stabilizing mechanism of highly oriented polyamide 6. *J. Therm. Anal. Calorim.* **2016**, *126*, 795–805. [CrossRef]
28. Do, C.H.; Pearce, E.M.; Bulkin, B.J.; Reimschuessel, H.K. FT–IR spectroscopic study on the thermal and thermal oxidative degradation of nylons. *J. Polym. Sci. Part A Polym. Chem.* **1987**, *25*, 2409–2424. [CrossRef]
29. Porubská, M.; Szöllős, O.; Kóňová, A.; Janigová, I.; Jašková, M.; Jomová, K.; Chodák, I. FTIR spectroscopy study of polyamide-6 irradiated by electron and proton beams. *Polym. Degrad. Stab.* **2012**, *97*, 523–531. [CrossRef]
30. Dong, W.; Gijsman, P. Influence of temperature on the thermo-oxidative degradation of polyamide 6 films. *Polym. Degrad. Stab.* **2010**, *95*, 1054–1062. [CrossRef]